Mechanics Research Communications 38 (2011) 1–11

Contents lists available at ScienceDirect

Mechanics Research Communications

journal homepage: www.elsevier.com/locate/mechrescom

Simulating fire effects on complex building structures☆

Howard R. Baum

Department of Fire Protection Engineering, University of Maryland, College Park, MD 20742, USA

ARTICLE INFO

Article history:
Available online 3 August 2010

Keywords:
Fire modeling
Heat transfer
Fire–structure interactions

ABSTRACT

The purpose of this lecture is to assess the current state of our ability to simulate the consequences of a fire in a large building, and suggest some areas where improvement is needed. Attention is focused on the coupling of fire dynamics simulations and heat transfer analyses to each other and to structural analyses of the damaged building. The role that uncertainty in "input parameters" resulting from coupling a sequence of complex simulations is considered. The methodology used in the NIST investigation into the collapse of the World Trade Center Towers will be described from this perspective. The intent is *not* to summarize the results of the investigation, but rather to provide a specific context that illustrates the strengths and weaknesses of the methodologies employed. Research needs are emphasized by examination of some basic problems in fire–structure interactions.

© 2010 Elsevier Ltd. All rights reserved.

1. Introduction

There has been a resurgence of interest in the response of building structures to fires over the past several years. This interest was greatly enhanced by the attack on, and subsequent collapse of, the World Trade Center (WTC) towers. This has resulted in at least three detailed physics-based analyses of the collapse of the towers in the literature. Usmani et al. (2003) and Hori (2004) concentrated on the degradation of the towers given assumed temperature distributions in the load bearing structures. Abboud et al. (2003) performed a more comprehensive analysis, dealing with both the initial impact of the aircraft as well as the final collapse, using as much photographic and video evidence as was available at the time (Beyler et al., 2003; Thater et al., 2003). More studies are surely on the way. NIST has just completed its own investigation, the details of which are available at the website http://www.wtc.nist.gov.

Rather than debate the causes of the collapse of the towers, it seems more useful at present to discuss the methodology used to study the collapse. Many if not most of the issues that had to be addressed in the WTC simulations would arise in the analysis of any major fire affecting the structural stability of a large building. The complexity of such buildings, together with the need to couple phenomena usually considered in isolation, forces compromises in methodology not required for simpler fire scenarios. This statement certainly applies to the analyses cited above, as well as the NIST investigation. Hopefully, the discussion will shed some new light on our ability to simulate such events.

First, the sequence of simulations of the consequences of the attacks on the towers and the software employed are discussed briefly. Very few details will be given, as the purpose is primarily to orient the reader. Since the software employed is widely available either as commercial products or NIST freeware, it is fair to assume it is representative of the current state of the art (indeed, it was chosen primarily for this reason). This is followed by a discussion of the approximations needed to couple the various elements of the simulation together. The role of fire-induced uncertainty and the extent to which the descriptions of the different physical processes must be coupled will be emphasized. A sampling of results (drawn primarily from the cited references) will be used to illustrate these points. The paper will conclude with some recommendations for future research. This work is an extended update of the Emmons Plenary Lecture presented by the author at the Eighth International Symposium on Fire Safety Science (Baum, 2005).

2. The NIST approach—a synopsis

The NIST-led analysis of the events initiated by the attack on the towers is composed of four parts; the initial impact, the fire dynamics, thermal analysis of the load-bearing structure, and structural deterioration. The information flow in principle proceeds as follows: The initial impact simulation is needed as input into the following three parts. It partially defines the geometry used for the fire dynamics simulation, provides guidance about insulation damage that affects the heat transfer calculation, and determines the state of the structure that survived the impact. The fire dynamics provides the thermal environment in the gas phase needed to determine the heat transfer to the exposed building surfaces. The thermal analysis determines the temperature distribution in the

☆ This paper discusses material that was presented in a lecture of the same title, the Elsevier/MRC Distinguished Lecture in Mechanics, at the New Jersey Institute of Technology, April 19, 2010.

E-mail address: hrbaum@umd.edu

0093-6413/$ – see front matter © 2010 Elsevier Ltd. All rights reserved.
doi:10.1016/j.mechrescom.2010.07.021

load bearing structure. Finally, the structural analysis integrates all the previous information to make predictions about the loads and deflections up to the point of collapse. The structural dynamics during the final collapse of the towers is not part of the investigation.

2.1. Impact analysis

Simulation of the initial impact of the aircraft on the towers, performed under contract, covers approximately the first 0.6 s of elapsed time. The simulations were performed using the commercial code LS-DYNA, "a general purpose finite element code for analyzing the large deformation dynamic response of structures including structures coupled to fluids" (Hallquist, 1998). It should be noted that although the code has some fluid mechanics simulation capability, it cannot simulate combustion phenomena. Thus, no attempt was made to simulate the initiation of the fireball in this part of the investigation. LS-DYNA and the finite element code FLEX (Vaughan, 2002) used by Abboud et al. share a common ancestor DYNA-3D, although both are undoubtedly much more capable now. The codes both used highly detailed representations of the aircraft structure and those floors of the WTC towers in the immediate vicinity of the impact to produce an estimate of the damage inflicted on the load bearing structure by the breakup of the aircraft.

The predicted damage to the exterior of the towers was verified by direct comparison with the highly detailed photographic and video evidence. The initial configuration, material properties, and relative velocity of both aircraft and building are known quite accurately. The level of sophistication in the computer codes then permits an impressively detailed prediction of the breach of the outer perimeter of the towers. However, the most important outputs of the analysis are the prediction of the post-impact interior geometry and the degree of damage to the insulation. For the purposes of the present paper, it completes the description of building needed for subsequent analyses. Thus, the remainder of this work will regard the post-impact state of the building as defined by these calculations as the initial conditions for the fire dynamics, thermal, and structural analyses.

2.2. Fire dynamics

The fires induced by the aircraft impact were studied using the NIST fire dynamics simulator (FDS), a finite difference based computational fluid dynamics code solving the low Mach number form of the Navier–Stokes equations appropriate for combustion, smoke and heat transport generated by fires (McGrattan, 2004). FDS was modified to enable parallel processing as part of this study (McGrattan and Bouldin, 2004). The code uses a geometry model of those floors of the towers affected by fires. The geometry model differs substantially from that used for the impact analysis, since it is based on architectural rather than structural features. The spatial resolution employed is too coarse to include much of the load-bearing structure, retaining only the floor slabs. The core and exterior columns are present but cannot be represented to scale. On the other hand, it includes the office partitions and work stations. The model also includes vents opened up either by estimates of damage caused by the initial impact or windows broken during the fire. Fig. 1 shows the geometry used by FDS. Every feature shown in the figure is included in the simulations. No attempt was made to predict window breaking. Photographic evidence was used to obtain times and locations of window breakage and the resulting information was specified as part of the input boundary conditions.

The fireballs resulting from the initial impact were studied separately to estimate the fuel consumed outside the towers and thus unavailable as an accelerant. Two independent techniques were used to obtain estimates of both the fuel consumption and the uncertainty of the estimate. FDS simulations were performed by Rehm et al. (2002) based on a variety of assumptions about the internal configuration of the towers following impact. Baum and Rehm (2005) performed an analytical study assuming the shape of the fireballs emerging from each face of the towers to be hemispherical. Comparison of these calculations with video images yielded estimates that 10–25% of the aircraft fuel was consumed.

The FDS simulations of the fires for the remaining life of the towers were tested by comparing predicted temperatures and heat release rates with those measured in a series of laboratory experiments. These experiments burned paper laden work stations similar to those used in the WTC towers in a compartment with limited openings resembling those in the towers. The actual office contents, their condition following the impact, and the completeness of burning are additional sources of uncertainty. Many simulations of the actual fires in the towers with varied assumptions about the input parameters were performed to test the sensitivity of the model. Calculated flame locations near the perimeter were compared with photographic and video images.

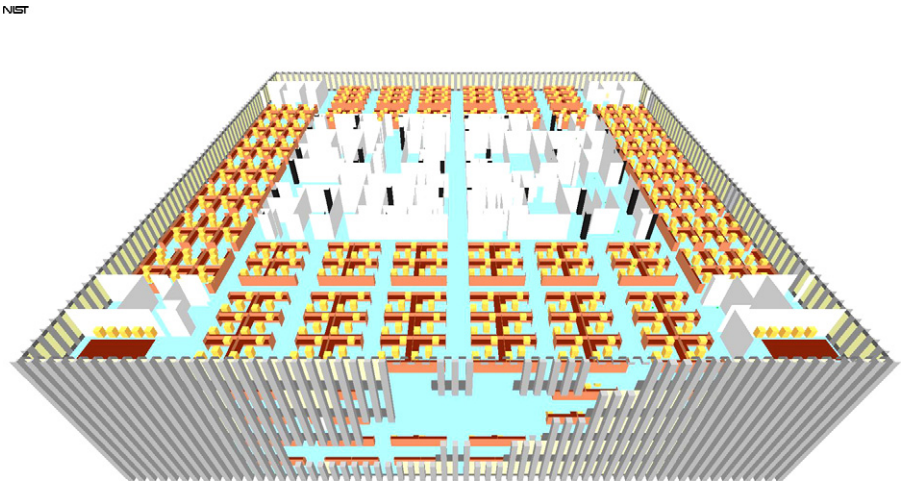

Fig. 1. Layout of North WTC tower model as used in FDS simulations. Windows, interior partitions, and workstation geometry are all included. However, the columns are not to scale and no internal floor system structural components are present in the simulations.
Courtesy McGrattan (2004)

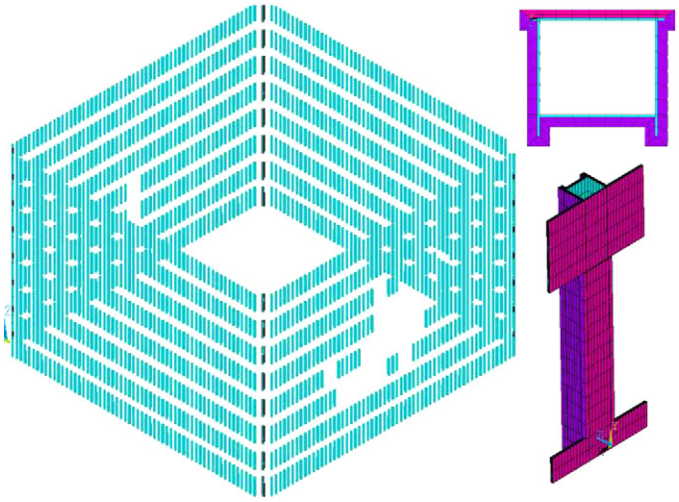

Fig. 2. The perimeter column structure of North WTC tower shown as simulated in the thermal analysis using ANSYS. The details of the column shapes and connection with spandrels are shown as inserts.
Courtesy K. Prasad (Baum, 2005).

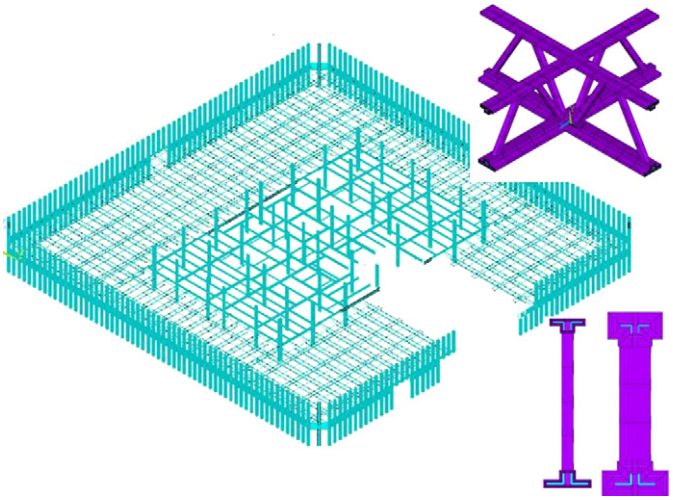

Fig. 3. The North WTC tower floor system (with concrete slab removed for clarity) and core columns shown as simulated in the thermal analysis using ANSYS. The details of the trusses including the insulation are shown as inserts. Additional illustrations can be found in Prasad and Baum (2005).
Courtesy K. Prasad (Baum, 2005).

Details of these and other aspects of the WTC fire simulations can be found in McGrattan and Bouldin (2004).

2.3. Thermal analysis

The thermal analysis of the structure couples the fire dynamics to the calculations of stress and deflection that ultimately determine the collapse path of the towers. The analysis itself is composed of two parts; the calculation of the local heat transfer from the heated gases to the exposed surfaces of insulation materials and structural components, and the heat flow through the condensed phase materials. A decision was made to use the code ANSYS (2003) to perform the structural analysis. Since ANSYS also has a thermal analysis capability, this led the development of a methodology that couples ANSYS to FDS. This methodology, the fire–structure interface (FSI), is capable of generalization to other codes and other structural fire problems. It makes use of a mixture of analytical and computational techniques to cope with the wide disparity of length and time scales that control the physical processes simulated in FDS and whatever structural analysis code is chosen for use. A more detailed description of the coupling procedures that comprise FSI is presented in the next section. These techniques are also summarized in Prasad and Baum (2005).

The finite element model used for the ANSYS simulation of the heating of the structure is the most detailed of all those used for the investigation. It is composed entirely of three-dimensional "brick" elements, and represents *all* the beams, columns, and floor systems on all floors affected by the fires (including the floors immediately above and below floors on which fires occured). It incorporates detailed models of the protective insulation, including estimates of damage obtained from calculated debris patterns performed as part of the impact analysis. Random irregularities in the thickness of spray-on insulation are also taken into account. Fig. 2 shows the perimeter columns and connections as simulated for the thermal analysis. The floor system and core columns are shown in Fig. 3. Analogous models were made for the South tower. The accuracy of the calculations was tested by comparing FSI predictions with a series of large scale experiments on steel trusses and columns. Studies of this type have been performed by Hasemi and his collaborators (Hasemi, 2000). The results indicate that FSI can reliably predict the temperature in structural components and that it does not add any more uncertainty to the overall analysis than that already present in the FDS simulations. A detailed analysis of the experimental uncertainty and model sensitivity associated with both the fire dynamics and thermal analysis of the laboratory experiments was also performed (Hamins et al., 2005).

This level of detail is necessary precisely because the calculations it supports provide the transition from large scale convective and radiative transport in the gas to highly localized thermal conduction through solids. It is also needed because it turns out that *the temperature distributions in the steel are more sensitive to the fireproofing thickness and the degree of impact damage to the insulation than any other quantity*. It is feasible only because heat transfer by thermal conduction (even non-linear conduction with non-linear radiative boundary conditions) is much simpler computationally than either turbulent combustion or non-linear solid mechanics.

2.4. Structural analysis

The stresses and displacements in the structure were calculated using ANSYS by a contractor with the thermal input from FSI and the initial impact damage estimate obtained from LS-DYNA. A series of highly detailed component models of relevant parts of the structure were subjected to a variety of loads. These were used to develop a less detailed set of floor-level models as well as multi-floor models of portions of the perimeter column system. Video images were used to select critical portions of the perimeter columns for detailed analysis. Finally, a global model based on simplifications derived from sensitivity analyses using the component and floor level models was developed. It should be noted that local models and/or highly simplified floor system models were also used by Usmani et al. (2003) and Hori (2004) in their analyses.

An interpolation scheme (part of FSI) was used to input the predicted temperatures into the finite element models employed for the structural analysis. The thermal information was transferred to the ANSYS structural model at intervals of 10 min of simulated time for each of the towers. Neither Usmani nor Hori attempted this step. This process introduces additional uncertainty into those calculations using the less detailed structural models, since it represents a loss of information calculated with FSI. However, it is crucial if a given fire scenario is to be associated with structural collapse. These issues will be discussed in further detail below.

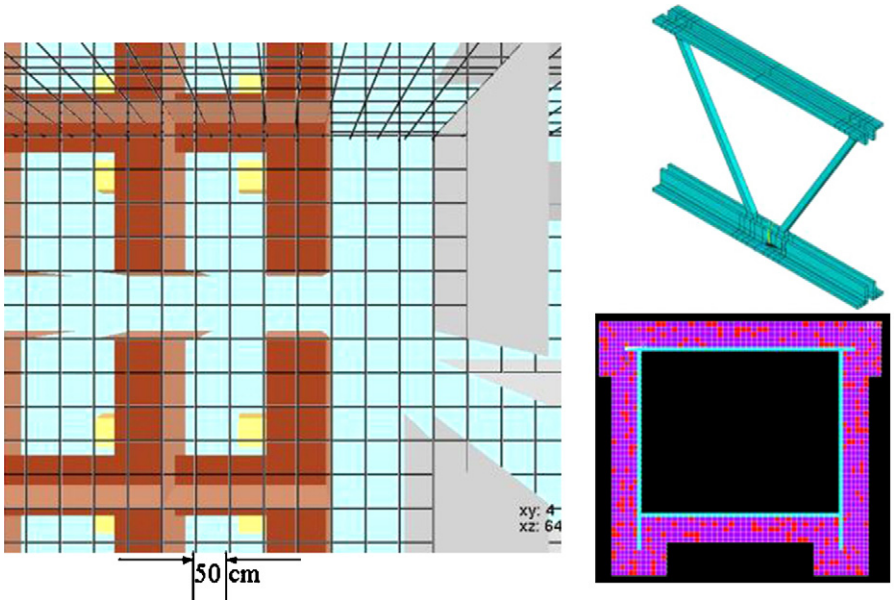

Fig. 4. Portion of WTC floor gridded at resolution used for FDS simulations. A section of the floor truss system and a perimeter column cross-section as modeled in ANSYS are also shown. The truss rods are 2.5 cm in diameter and the column is 35 cm on a side.
Courtesy K. Prasad (Baum, 2005).

3. Coupling and feedback

The sections above outline how the overall analysis was broken down and indicate the methods used to study each portion of the overall simulation as an isolated entity. However, if the effects of a given fire on a structure are to be predicted, it is necessary to couple these codes in an internally consistent manner. Since the aircraft impact is both peculiar to the WTC attack and considers less than 1 s of elapsed time, attention is focused on the interactions between the fire dynamics, heat transfer, and structural analysis. These processes occur simultaneously in reality, but are considered sequentially in the WTC analyses. This is a reflection of the current state of the art. I can find no published example of a fully coupled simulation of a fire in a complex structure that includes fire dynamics, heat transfer, and structural mechanics.

At many points in the WTC analyses, photographic and visual evidence are used to compensate for our current inability to perform a fully coupled simulation. The most obvious of these is the effect of window breaking on fire dynamics. While glass windows are not structural components, the "collapse analysis" of such a window requires a coupling of fire dynamics, heat transfer and stress analysis analogous to that needed for the load bearing structure. Fortunately, there is no need to consider this problem in detail since it was the subject of a superb recent review by Pagni (2003). From the present perspective, the most important conclusion to emerge from this review is the following: While the time to initial crack formation in the glass can be reliably estimated as a function of window geometry, materials, and thermal load, the time at which the glass falls out of its frame cannot be predicted with any confidence. Since the fire ventilation will not change until the window pane is removed from its frame, this aspect of the feedback from changes in the building structure to the fire can not yet be quantified.

3.1. The fire–structure interface

The coupling between the fire dynamics and the structure is dominated by the radiation heat transfer. The radiation field must be determined from solutions of the radiative transport equation, which relates the incident flux to the spatial distribution of temperature and combustion products (most particularly the distribution of soot particulate) as well as the enclosure geometry. Such calculations are typically performed as part of a CFD based simulation of the fire dynamics. However, the ability to couple such codes as the NIST Fire Dynamics Simulator (FDS) McGrattan (2004) directly to a suitable structural analysis code does not yet exist. The enormous differences in spatial and temporal length scales, differences in numerical techniques, and the complexity of the computer codes makes the development of an efficient coupled analysis of fire–structure interactions a daunting task. This disparity in length scales is illustrated in Fig. 4, which shows a small portion of a WTC floor gridded at the 50 cm resolution used for the FDS simulations together with a small segment of the floor truss system and an insulated perimeter column as represented in ANSYS. Since the truss rods have a 2.5-cm diameter and the perimeter columns are 35 cm on a side it is clear that FDS must be supplemented by a method that permits the heat transfer to the structure to be calculated.

The FSI offers an approach to the calculation of the coupled heat transfer problem. It takes advantage of the fact that the simplest compartment fire models, the "zone models", assume that the compartment is divided into a hot, soot laden upper layer and a cool, relatively clear lower layer. For the purposes of the FSI, the temperature gradients in the horizontal directions are much smaller than those in the vertical direction. The layer temperatures and radiative properties are taken from suitably chosen temporal and spatial averages of output generated by FDS. The time averages are chosen to be compatible with the time scales associated with thermal diffusion through the smallest structural members of interest. The spatial averages replace the detailed vertical temperature and absorption coefficient profiles with an effective "zone model" profile. This last approximation is not crucial to the development of the FSI, but is used to reduce the information transfer required between FDS and ANSYS.

The step that *is* crucial is recognition of the implications of the layered thermal and optical properties of the gas phase. Let length scales in the horizontal directions $\bar{x}$ be scaled with a length L (over

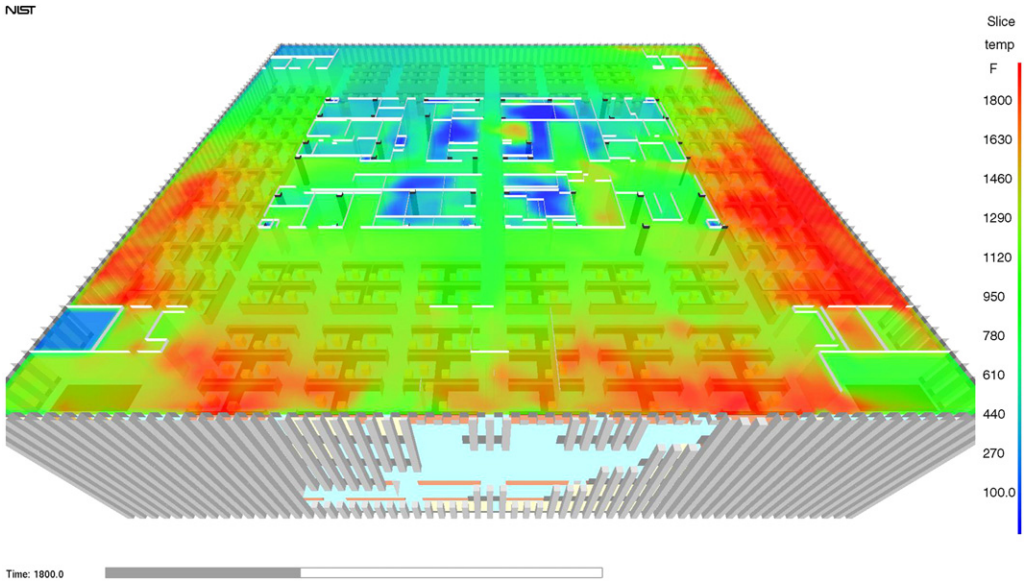

Fig. 5. Predicted upper layer temperature of a floor of the north tower 30 min after impact using the model shown in Fig. 1 . The peak temperatures are in the vicinity of 1100 °C.
Courtesy McGrattan (2004)

60 m in the WTC towers), while the grey gas absorption coefficient κ and length scales in the vertical direction z are scaled with H, the height of an individual floor (less than 4 m in the WTC towers). Finally, let the integrated intensity $I(\vec{x}, z, \vec{\Omega}_x, \Omega_z)$ be normalized with respect to σT_r^4, where σ is the Stefan–Boltzmann constant, $\vec{\Omega} = (\vec{\Omega}_x, \Omega_z)$ denotes the local direction of the radiation field, and T_r a suitable reference temperature. Then, denoting dimensionless quantities with a tilde, the radiative transport equation takes the form:

$$\frac{H}{L}(\vec{\Omega}_x \cdot \nabla_x \tilde{I}) + \Omega_z \frac{\partial \tilde{I}}{\partial z} = \tilde{\kappa}\left(\frac{(\tilde{T})^4}{\pi} - \tilde{I}\right) \quad (1)$$

Since the ratio $H/L \ll 1$, the terms in round brackets on the left hand side of Eq. (1) can be ignored. The remaining terms are those associated with the problem of radiative transport between plane parallel layers. For this simplified geometry, the radiative transport equation can be solved exactly and explicit formulae for the heat flux obtained as functions of the temperatures, hot layer depth, soot concentration, as well as the location and orientation of the structural element. The basic analysis is quite well known in the heat transfer community (Siegel and Howell, 1992), and the extensions needed for use in FSI are readily obtained. Details can be found in Prasad and Baum (2005).

The FSI converts these formulae into input for ANSYS or any other finite element computer code that can be used for both time dependent three dimensional heat transfer within the solid phase and for the stress analysis of the heated structure. The solid phase heat transfer is dominated by thermal conduction with thermal radiation boundary conditions. The input radiation is calculated by FSI based on averages extracted from FDS, while the outgoing radiation is a function of the surface temperatures predicted by ANSYS. A very detailed geometry model of all solids can be accommodated, with solutions that account for insulation damage as well as statistical variations in the application of spray-on fireproofing. Finally, the FSI interpolates the temperatures obtained from this calculation into the geometry model employed for the stress analysis. The complexity of the structural mechanics simulations makes this last step necessary.

3.2. Sample simulations

As noted above, the simulations are performed sequentially, with the FDS simulation coming first. Fig. 5 shows a snapshot of the upper layer temperatures in the north tower 30 min after impact (McGrattan, 2004). This was one of a series of development simulations, and is not necessarily the best prediction of the state of the fires at that time. However, it gives a general idea of the kind of predictions that can be made using this methodology. Note that the fire dynamics on *all* floors must be computed simultaneously, since the floors are connected by both ventilation shafts and impact damage. The results show fires that slowly migrate around the floor, with peak temperatures in the upper layer in the vicinity of 1100 °C. Fig. 5 also shows the relatively smooth temperature variation over most of the upper layer with rapid transitions confined to the edges of the high temperature zones where burning is taking place. This helps justify the plane layer radiative transport analysis used by the FSI.

The computational mesh, even at 50 cm resolution, requires nearly 150,000 cells per floor. Over 500,000 time steps are needed to advance the calculation for 6000 s of simulated time. Without the use of the parallel processing technique incorporated into FDS as part of the WTC investigation, these calculations would be nearly impossible to perform. Indeed, McGrattan (2004) estimate that the computation illustrated in Fig. 5 would take up to 2 months on a single processor, if it were capable of addressing the 6–12 gigabytes of memory required to perform the computation. This memory requirement would rule out the use of all 32 bit "commodity" processors. The use of parallel processing has reduced the time needed to complete a simulation to as little as two days using eight processors per floor. Moreover, by breaking up the calculation so that the computational demands on each processor are not too large, inexpensive commodity processors in "Beowulf Clusters" connected with gigabit networks can be employed.

Since the time step used by FDS is of order 0.01 s, and the smallest time scales of interest in the thermal analysis are several seconds, only averaged values of T^4 and the absorption coefficient at several second intervals need be passed from FSI to ANSYS. It also opens the possibility of coupling the fire and thermal analyses together. So long as hundreds of FDS updates can be performed

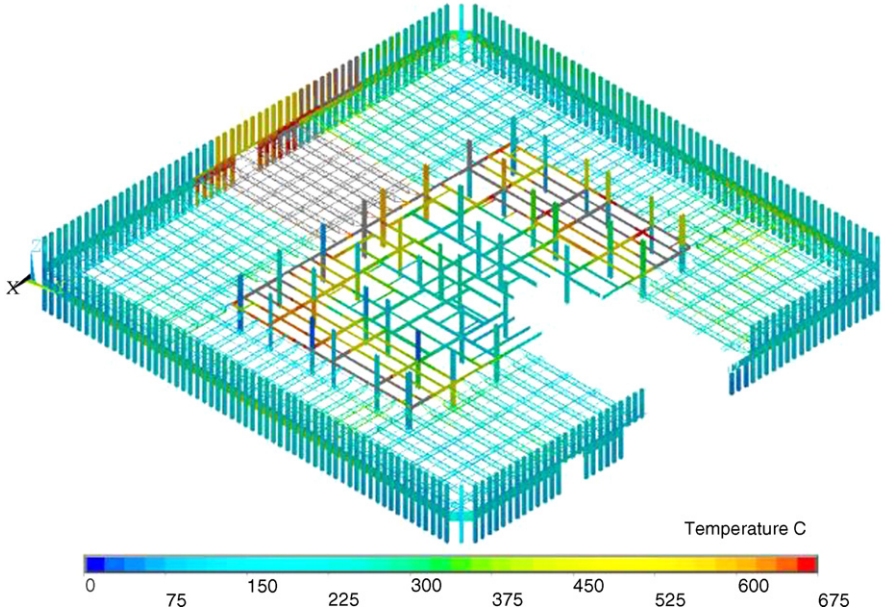

Fig. 6. Predicted temperatures in the steel structure of the 96th floor of the north tower 100 min after impact. The peak temperatures reach 675 °C. The calculation for each floor includes the insulation and concrete slab (not shown).
Courtesy K. Prasad (Baum, 2005).

between solid phase thermal updates, the cost of restarting FDS with a corrected set of thermal boundary conditions derived from the solid phase analysis can be minimized. This issue will be addressed again below.

Predicted temperatures in the steel structural components of the 96th floor of the north tower 100 min after impact are shown in Fig. 6. This is one of a series of development simulations, and is not necessarily the best prediction of either the thermal or mechanical state of the structure at that time. However, it does illustrate the extent to which the FSI permits highly detailed calculations of the thermal state of the structure to be coupled with FDS simulations. The peak temperatures in this simulation reach 675 ° C near the south face of the floor, opposite the damaged portion of the floor. This is roughly the area reached by the fires several minutes earlier as they moved about the floor. The simulation includes the concrete slab and the insulation material, which are omitted for clarity.

The above simulation spans a range of length scales ranging from over 60 m (the tower width) to 1 cm (the radius of a truss rod). The entire floor system of each individual floor, including insulation and the concrete floor slab, is coupled together in a single calculation. The ANSYS model for a single combined floor system contains approximately 450,000 nodes and 650,000 elements (Prasad and Baum, 2005). Each column is simulated separately, since they are weakly coupled thermally. The column models have 20 nodes per floor in the vertical direction and a few hundred to describe the heat transfer in each horizontal cross section. Thus, the number of nodes and elements in the columns is comparable to that in the floor system. It takes approximately one day per floor to perform a thermal analysis. Clearly, calculations at this level of detail are only possible because of the relative simplicity of conduction heat transfer compared with turbulent combustion. The fact that each floor can be simulated independently is itself a form of parallel processing. It requires many copies of the simulation code (ANSYS in this case), as opposed to a single copy of FDS for the fire simulations. However, financial issues aside, it leads to highly efficient computations.

The efficiency of the computations is of more than passing interest. Given the propagation of uncertainty through the chain of simulations, it is not possible to obtain credible results without many repetitions of each calculation. Only in this way can the sensitivity of the calculations to plausible variations in input be established. Moreover, the only way to make contact with the photographs and videos that provide a check on the credibility of the simulations is to repeat them enough times to establish the plausibility of the results. Tens of calculations of the type illustrated in the figures shown here have been performed as part of the NIST WTC investigation.

One novel feature of the thermal analysis performed by the FSI is worth special mention. The thickness of the spray-on insulation on the trusses in the WTC towers has been the focus of considerable attention (Quintiere et al., 2002). However, given the method of application, the thickness can only be defined statistically, as there is a wide variation in the actual thickness at each point along the protected components. Fig. 7 illustrates the methodology developed to deal with this fact. An artificially thick uniform insulation model is built up around each protected rod. Then a mean thickness and variance are chosen, and individual elements are chosen statistically to have either the proper thermal properties or essentially no thermal inertia. The result is a finite element model whose geometric simplicity is preserved but which accounts for the loss of protection associated with random thickness variations. The result is a net loss for a given average thickness because those portions of the rod with less protection experience higher heat transfer. The excess heat can be transferred a small distance along the rod by axial diffusion, canceling whatever reduction might have resulted from the thicker adjacent insulation. This also gives rise to local "hot spots", which can cause a weakening of the structural element in the immediate vicinity of the spot.

4. Research issues

The remaining issues to be discussed here concern the coupling between the thermal analysis of the structure and the calculation of stress and displacement fields. While they may not be "research issues" in the strictest sense of the word, the extent to which these phenomena need to be coupled is not adequately appreciated in the view of this author. The first point worth emphasizing is that the spatial and temporal resolution of the stress analysis cannot be

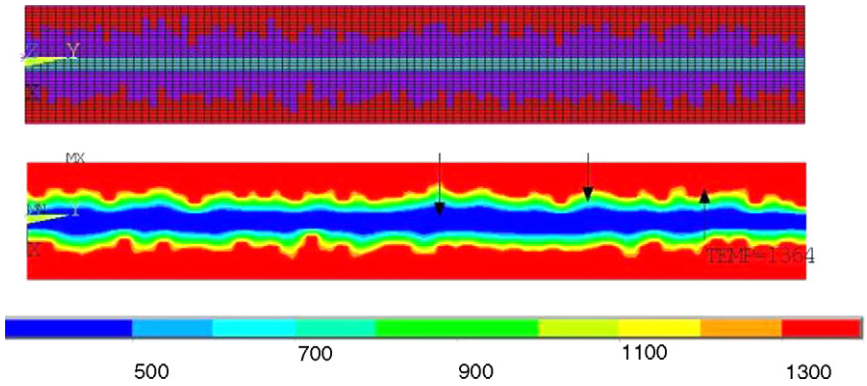

Fig. 7. Finite element model of spray-on insulation showing random variations in thickness (top). The outer layer of cells have no thermal inertia, the middle layer represents the actual insulation whose thickness is specified statistically, and the inner layer simulates the steel rod. The lower figure shows the computed temperatures.
Courtesy K. Prasad (Baum, 2005).

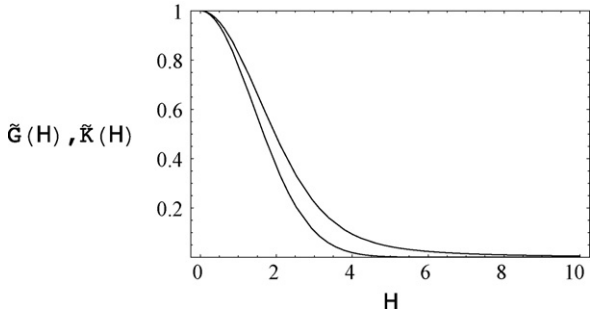

Fig. 8. Kernel functions normalized by their value at $\eta = 0$. The quantities actually plotted are $\tilde{G}(\eta) = G(\eta, \tau)/G(0, \tau)$ and $\tilde{K}(\eta) = K(\eta, \tau)/K(0, \tau)$. The Gaussian function G decays more rapidly than K which decays $\sim\eta^{-3}$.

chosen arbitrarily once the requirements for thermal analysis have been decided.

Consider the idealized problem of a three-dimensional elastic half-space that is loaded thermally by a moving point source of heat $q_o Q_T(\tau)$ concentrated at a point on the free surface $\vec{r} = \vec{R}(\tau)$. Then, the classic theory of linear thermo-elasticity can be used to show that without approximation the surface temperature rise and the normal component of the surface displacement (the "bulge") take the following form (see Fig. 8):

$$\Theta(\vec{r}, \tau) = \int_0^\tau d\tau_o Q_T(\tau_o) G(\tau - \tau_o, \eta_T)\eta_T = \frac{\left|\vec{r} - \vec{R}(\tau_o)\right|}{\sqrt{(\tau - \tau_o)}} \tag{2}$$

$$w(\vec{r}, \tau) = \int_0^\tau d\tau_o Q_T(\tau_o) K(\tau - \tau_o, \eta_T)\eta_T = \frac{\left|\vec{r} - \vec{R}(\tau_o)\right|}{\sqrt{(\tau - \tau_o)}} \tag{3}$$

Here, G is the classical Gaussian Kernel function and K is an analogous function that emerges from the thermo-elastic analysis. The variable τ is a time normalized with the time scale t_o imposed by the thermal heating, and the length scale $l = \sqrt{t_o/\alpha}$ where α is the thermal diffusivity. The dimensionless temperature rise Θ is made non-dimensional with respect to $q_o l/k$, where k is the thermal conductivity. The surface displacement w is normalized by l and a thermo-elastic "coupling constant". The function K can be written explicitly as:

$$K = -\left(\frac{2\mu + \lambda}{\mu + \lambda}\right)\frac{1}{8\pi\tau}\ \exp\left(\frac{-\eta^2}{8}\right)\left(I_o\left(\frac{\eta^2}{8}\right) - I_1\left(\frac{\eta^2}{8}\right)\right) \tag{4}$$

The quantities λ and μ are the Lamé constants of classical elasticity, while I_0 and I_1 are Modified Bessel functions. These results are probably well known, although I cannot find them in the classical literature. A derivation of these results is presented in the appendix.

The importance of these formulae lies in the fact that both the temperature rise and displacement are shown to be inherently time-dependent diffusive processes, with the time scale and diffusion set by the temperature field. Moreover, the displacements depend explicitly on the entire space-time history of the thermal heating of the exposed surface. If the temperature field is independent of time or if it is postulated as opposed to derived, then this issue does not arise. However, under either of these circumstances, it is no longer possible to couple the fire dynamics to the structural analysis. While the problems of interest in a structural collapse scenario are inherently non-linear, that does not invalidate the above conclusions. The thermally induced diffusion is then superimposed on a variety of other phenomena.

The significance of geometric non-linearity caused by large thermally induced displacements has recently been emphasized by Lane (2003). This has important consequences for coupled thermal-structural analyses. Even if large deflections in components of the structure do not change the fire dynamics appreciably, the deformation can change the thermal environment experienced by the component. Fig. 9 shows a comparison between two time dependent ANSYS simulations of a horizontal rod fixed at the ends and placed in a gas with a temperature distribution that increases with increasing height. The simulation on the left assumes the heat transfer to the rod is evaluated at its original position while the right hand simulation uses the current position of the rod. The

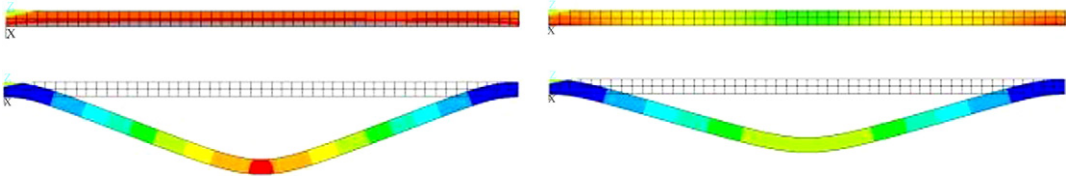

Fig. 9. Temperatures (top) and displacements of an unprotected steel rod in a gas with a vertically stratified temperature profile. The simulation on the left assumes the heat transfer to the rod is evaluated at its original position while the right hand simulation uses the current position of the rod.
Courtesy K. Prasad (Baum, 2005).

upper part of the figure shows the temperatures while the deflections are shown below. Note that the temperature in the left hand simulation is uniform, because the heat flux to the rod is always evaluated at the original location, even though the temperature in the rod increases with time. The change in heat flux to the rod with changing location is included in the right hand simulation. As a result, the rod temperature varies significantly with position. The deflections in this case are smaller, because as the rod deforms it moves into a cooler environment with lower heat transfer as a result. While this may not seem too important for an isolated truss rod, the consequences if repeated on a large scale can be quite significant (Usmani et al., 2003; Lane, 2003). Both effects illustrated in this section could be addressed if thermal and stress analyses of a given structure were performed in parallel rather than sequentially. The difficulty arises in choosing a consistent level of modeling detail which preserves the ability to perform the stress analysis without compromising the accuracy of the temperature field.

5. Concluding remarks

A discussion of the current state of our ability to predict the effects of fire on building structures has been presented. The emphasis has been on the degree to which fire dynamics, heat transfer, and structural analysis can be coupled. The NIST investigation into the collapse of the WTC towers is used as a backdrop, because it provides a concrete illustration of the strengths and limitations of our current methodology. While the simulation capability in each of these fields can (and no doubt will) be advanced separately, it is only when they are coupled together in some way that fire effects on structures can be quantitatively assessed. This is an area that would benefit greatly from increased attention by the Fire Research community. I hope this community will rise to the challenge.

Appendix A. Thermal stress analysis

A.1. Background

The following analysis is motivated by the observation that the calculation of stresses induced by time dependent temperature fields using certain commercial software packages seems to be much more difficult than the corresponding calculation for an isothermal environment. While the applications of interest clearly involve highly non-linear calculations, the starting point for most fire scenarios is almost always an undamaged building at room temperature. Since virtually all buildings are designed to keep the stresses well below the elastic limit and the deflections of the load bearing structure reasonably small, the starting point for simulations of fire induced damage *must* lie within the domain of *linear* elasticity. Moreover, the difficulties that arise using the packages of interest are evident before the temperature rise is large enough to affect the elastic or thermal properties of most structural materials. Under these circumstances the thermally induced stresses are also linear, and the temperature fields can be described by the heat conduction equation for the material(s) of interest.

The facts described above justify an analysis of the coupling between the temperature and thermally induced stresses based on the *linear* thermo-elastic equations. The temporal dependence of the stresses is the focus of this analysis. A popular technique for solving the thermo-elastic equations is to first compute (or assume) the time dependent temperature distribution in the load bearing structure. Then, given this information, the temperature distributions are "frozen" at a succession of discretely chosen times and an equilibrium solution is sought for the state of stress at each chosen time. The fact that the temperature is changing continuously and that this continuous change *must* affect the stresses is ignored in this approach. This technique is justified by noting that the elastic wave propagation speed is so fast compared with the time scales of interest in thermo-elastic phenomena induced by fires that a quasi-steady analysis is justified.

The analyses that follow are intended to show that computational techniques that "freeze" the temperature at a given time and compute an equilibrium stress distribution are not consistent with the dynamical equations of thermo-elasticity, even if the elastic wave propagation speed is taken to be infinite. The next section demonstrates how the general solutions to the equations of thermo-elasticity couple the time scale for the evolution of the displacements to that of the temperature field. In particular, it is shown that the solutions for the displacements cannot obey an equilibrium equation unless the temperature field is independent of time. Following this, formal solutions for a half-space loaded thermally are derived. Again, it is clear that part of the solution for the stresses and displacements are inherently time dependent.

A.2. The thermo-elastic equations

The starting point for the analysis are the linear thermo-elastic equations which relate the displacements u_i and stresses τ_{ij} to each other and to the temperature T in the elastic medium. They can be written in the form Sokolnikoff (1956):

$$\rho\frac{\partial^2 u_i}{\partial t^2} = F_i + \frac{\partial \tau_{ij}}{\partial x_j} \tag{A.1}$$

$$\tau_{ij} = \lambda\frac{\partial u_k}{\partial x_k}\delta_{ij} + \mu\left(\frac{\partial u_i}{\partial x_j} + \frac{\partial u_j}{\partial x_i}\right) - \alpha(3\lambda + 2\mu)(T - T_o)\delta_{ij} \tag{A.2}$$

Here, ρ is the density of the material, F_i is the body force per unit volume, μ and λ the Lamé constants, α the coefficient of thermal expansion, and T the temperature. The temperature T_o is the reference temperature of the material in its unstressed state before the fire. That temperature is taken to be uniform here, which is a reasonable simplification given the temperature rise associated with a building fire. These equations are supplemented by suitable boundary conditions that express the connections to other portions of the structure and external loads. The temperature field evolves according to the heat conduction equation.

$$\rho C_p\frac{\partial(T - T_o)}{\partial t} = k\frac{\partial^2(T - T_o)}{\partial x_k^2} \tag{A.3}$$

The coupling between the stresses and the temperature field comes from the effect of the temperature gradients on the volumetric expansion ϕ. The body force plays no role in this and will henceforth be ignored. Taking the divergence of the thermo-elastic evolution Eq. (A.1) yields:

$$\phi \equiv \frac{\partial u_k}{\partial x_k} \tag{A.4}$$

$$\rho\frac{\partial^2 \phi}{\partial t^2} = (\lambda + 2\mu)\nabla^2\phi - \alpha(3\lambda + 2\mu)\nabla^2(T - T_o) \tag{A.5}$$

The next step is to simplify these equations by eliminating the fast wave motion associated with the irrotational waves. It is easy to see from Eq. (A.5) that these waves propagate with a speed $c^2 = (\lambda + 2\mu)/\rho$. For typical steels, $c \sim O(10^3)\,m/s$. Moreover, the thermal diffusivity $k/(\rho C_p) \sim O(10^{-5})\,m^2/s$. We now introduce dimensionless thermal and mechanics variables respectively as follows:

$$T - T_o = \left(\frac{q_o l}{k}\right)\Theta(y_i, \tau), \quad x_i = l y_i, \quad t = t_o\tau, \quad l = \sqrt{\frac{k t_o}{\rho C_p}} \tag{A.6}$$

$$\phi = \beta\Phi(y_i, \tau), \quad u_i = \beta l v_i, \quad \beta = \alpha q_o \sqrt{\frac{t_o}{k\rho C_p}} \left(\frac{3\lambda + 2\mu}{\lambda + 2\mu}\right) \tag{A.7}$$

$$\epsilon^2 = \frac{k}{C_p t_o} \frac{1}{(\lambda + 2\mu)} \tag{A.8}$$

The non-dimensional variables are chosen so that the full time dependent heat conduction equation is retained, and the temperature rise is related to a heat flux to a bounding surface q_o. The coupling parameter β scales the thermally induced deformations to the temperature rise, and ϵ is the ratio of the speed of a thermal "front" to the irrotational wave speed in the elastic medium. The time scale t_o is arbitrary, and its choice sets both the diffusion controlled length scale and the magnitude of ϵ. Given the approximate values of wave speed and thermal diffusivity shown above, it is clear that $\epsilon \ll 1$ for any time scale of interest in a fire scenario.

The dimensionless evolution equations for the normalized dilation Φ and temperature rise Θ take the following form:

$$\frac{\partial \Theta}{\partial \tau} = \nabla^2 \Theta \tag{A.9}$$

$$\epsilon^2 \frac{\partial^2 \Phi}{\partial \tau^2} = \nabla^2 \Phi - \nabla^2 \Theta \tag{A.10}$$

$$\Phi = \nabla \cdot \vec{v} \tag{A.11}$$

It is now easy to show the structure of the solution for the irrotational portion of the deformation. Ignoring terms of order ϵ^2, it is clear that Φ *must* have the form:

$$\Phi = \Theta + \Phi^*, \quad \nabla^2 \Phi^* = 0 \tag{A.12}$$

This clearly shows that the dilation has two parts: a harmonic contribution Φ^* that can be regarded as a local equilibrium solution corresponding to the instantaneous boundary conditions, and a part that is directly proportional to the local temperature rise. This part of the solution *never* is in equilibrium, unless the temperature is in steady state. While a steady temperature field may be a useful approximation to the state of a furnace, for example, it is a very poor representation of the temperature distribution resulting from a building fire.

This result can be seen even more clearly by noting that since the dimensionless displacement is a vector field, it can always be decomposed into an irrotational and a solenoidal part.

$$\vec{v} = \nabla \Psi + \nabla \times \vec{A} \tag{A.13}$$

Then, since $\nabla \cdot \vec{v} = \Phi = \nabla^2 \Psi$, the scalar potential function Ψ satisfies the equation:

$$\nabla^2 \Psi = \Theta + \Phi^* \tag{A.14}$$

The harmonic function Φ^* can be eliminated to obtain an explicit relation between the irrotational component of the displacement and the temperature field in the following form:

$$\nabla^2 \nabla^2 \Psi = \frac{\partial \Theta}{\partial \tau} \tag{A.15}$$

Here, the fact that Θ satisfies the heat conduction equation has been used. Alternatively, the solution for Ψ can be decomposed into an evolution equation and an equilibrium equation as follows:

$$\Psi = \Psi^* + \Psi_1 \tag{A.16}$$

$$\nabla^2 \nabla^2 \Psi^* = 0, \quad \left(\frac{\partial}{\partial \tau} - \nabla^2\right) \nabla^2 \Psi_1 = 0 \tag{A.17}$$

Both Eqs. (A.15) and (A.17) show that only part of the solution for the thermally induced displacement can correspond to a local equilibrium state if the temperature varies with time. Any solution procedure that works by "freezing" the temperature in time and using an equilibrium equation to satisfy the boundary conditions *must* miss at least part of the solution to the equations of thermoelasticity. Eq. (A.15) shows that when the temperature is "frozen", the right hand side of the equation is replaced by zero over almost all time, except at the discrete points where a Dirac delta function is in effect used to update the temperature field. The accuracy of this kind of approximation is completely unknown. Eq. (A.17) shows that the non-equilibrium portion of the solution evolves on the same time scale as the solution to the heat conduction equation. Moreover, since the heat conduction solutions are smooth, the solution to the non-equilibrium displacement field must also be smooth. This would seem to rule out approximating the time dependence of the temperature field by a discrete set of steps for the purpose of calculating the displacement fields.

A.3. Heated elastic half-space

In order to make some of these ideas more precise, consider the idealized problem of an elastic half-space heated at the surface by a prescribed heat flux that in general depends on space and time. The variables are made dimensionless as before, with the coordinate normal to the surface pointing *into* the solid denoted by z, and the coordinates parallel to the surface denoted by $\vec{r} \equiv (x, y)$. The *dimensional* heat flux to the surface at $z = 0$ is given by $q_z = q_o Q(x, y, \tau)$. Furthermore, body forces are ignored and there are no mechanical forces acting on the surface $z = 0$. Thus, the only reason any stresses and deformations are set up in the solid is because of the thermal loading.

Under these circumstances, the boundary conditions at the surface become:

$$\tau_{zi} = 0, \quad i \equiv x, y, z; \quad \frac{\partial \Theta}{\partial z} = -Q(x, y, \tau) \tag{A.18}$$

The stress free boundary conditions can be conveniently rewritten in terms of displacements by introducing the parallel displacement vector $\vec{V} \equiv (u, v)$, the perpendicular displacement w, and the parallel gradient operator ∇_h defined by:

$$\nabla_h \equiv \left(\frac{\partial}{\partial x}, \frac{\partial}{\partial y}\right) \tag{A.19}$$

The requirement that the two shear components of the stress vanish at the surface can then be written in the form:

$$\nabla_h w + \frac{\partial}{\partial z} \vec{V} = 0 \quad @z = 0 \tag{A.20}$$

Similarly, the normal stress will vanish at the surface provided that:

$$\lambda \Phi + 2\mu \frac{\partial w}{\partial z} = (\lambda + 2\mu)\Theta \quad @z = 0 \tag{A.21}$$

In the present notation, Φ can be written in the form:

$$\Phi = \nabla_h \cdot \vec{V} + \frac{\partial w}{\partial z} = \Theta + \Phi^* \tag{A.22}$$

The heat flux is assumed to be applied to the surface over a finite area. Thus, the temperature rise together with all displacements must vanish as $z \to \infty$ and $\vec{r} \to \infty$.

The equations that must be solved can now be rewritten as follows. The heat conduction equation takes the form:

$$\frac{\partial \Theta}{\partial \tau} = \left(\nabla_h^2 + \frac{\partial^2}{\partial z^2}\right) \Theta \tag{A.23}$$

Using the general results obtained in the previous section, the equilibrium equations for the parallel components of the displacement become:

$$\left(\nabla_h^2 + \frac{\partial^2}{\partial z^2}\right) \vec{V} + \left(\frac{\mu + \lambda}{\mu}\right) \nabla_h \Phi^* = \nabla_h \Theta \tag{A.24}$$

The auxiliary function Φ^* defined in Eq. (A.12) satisfies the Laplace equation, written in the present notation as:

$$\left(\nabla_h^2 + \frac{\partial^2}{\partial z^2}\right)\Phi^* = 0 \tag{A.25}$$

The system of equations that must be solved thus consists of Eq. (A.23), which determines Θ, Eq. (A.24), which determines $\bar{V}$, Eq. (A.25), which determines Φ^*, and Eq. (A.22), which determines w.

The solutions can be obtained using transform methods. Let the Fourier–Laplace transform of an arbitrary function $f\left(\vec{r}, z, \tau\right)$ be defined as follows:

$$\bar{f}\left(\vec{k}, z, p\right) = \int_{-\infty}^{\infty} d^2\vec{r} \int_0^{\infty} d\tau \;\; \exp(-i\vec{k}\cdot\vec{r} - p\tau) f(\vec{r}, z, \tau) \tag{A.26}$$

The Fourier–Laplace transform of the solutions satisfying boundary conditions at infinity can then readily be found to be:

$$\bar{\Theta} = \bar{Q}(\vec{k}, p)\frac{\exp\left(-\sqrt{p+k^2}z\right)}{\sqrt{p+k^2}} \tag{A.27}$$

$$\overline{\Phi^*} = \bar{A}(\vec{k}, p)\exp(-kz) \tag{A.28}$$

$$\bar{\vec{V}} = i\vec{k}\bar{\Psi}(\vec{k}, p) \tag{A.29}$$

$$\bar{\Psi} = \bar{\Theta} + \bar{B}(\vec{k}, p)\exp(-kz) + \left(\frac{\mu+\lambda}{\mu}\right)\bar{A}(\vec{k}, p)\frac{z}{2k} \;\; \exp(-kz) \tag{A.30}$$

$$\bar{w} = -\frac{\bar{Q}}{p}\exp\left(-\sqrt{p+k^2}z\right) - k\bar{B} \;\; \exp(-kz) - \omega\bar{A} \;\; \exp(-kz) \tag{A.31}$$

$$\omega = \frac{3\mu + \lambda + (\mu+\lambda)kz}{2k\mu} \tag{A.32}$$

The unknown functions $\bar{A}(\vec{k}, p)$ and $\bar{B}(\vec{k}, p)$ are determined by the surface boundary conditions given in Eqs. (A.20) and (A.21). The results are:

$$\bar{A} = \left(\frac{\mu}{\mu+\lambda}\right)\frac{2k\bar{Q}}{p}\left(1 - \frac{k}{\sqrt{p+k^2}}\right) \tag{A.33}$$

$$\bar{B} = \frac{\bar{Q}}{(\mu+\lambda)p}\left(\frac{\mu}{\sqrt{p+k^2}} - \frac{2\mu+\lambda}{k}\right) \tag{A.34}$$

Since the primary interest in this solution is the extent to which the time dependence is imbedded in the result, attention is focused on the vertical displacement at the surface. This part of the solution can be readily obtained and interpreted in the light of the general formulation discussed in the previous section. Physically, it represents the "bulge" in the surface that would appear in the vicinity of the heated area. The recipe for the bulge can be readily compared with that for the temperature rise at the surface induced by the heat transfer. Since it is well known that the temperature distribution *must* be treated as a transient phenomenon, the similarities and contrasts between these two results will lend insight into the importance of a coupled transient analysis of the stresses and displacements induced by the heat transfer.

First consider the surface temperature distribution. Using the convolution theorem, the solution can be written in the form:

$$\Theta(\vec{r}, \tau, 0) = \int_0^{\tau} d\tau_o \int_{-\infty}^{\infty} d^2\vec{r}_o Q(\vec{r}_o, \tau_o) G(\vec{r} - \vec{r}_o, \tau - \tau_o) \tag{A.35}$$

$$G(\vec{r}, \tau) = \frac{1}{4(\pi\tau)^{3/2}}\exp\left(\frac{-\eta^2}{4}\right), \quad \eta = \frac{r}{\sqrt{\tau}} \tag{A.36}$$

In order to simplify the analysis, consider the special case where $Q(\vec{r}, \tau)$ is concentrated at a point $\vec{r} = \vec{R}(\tau)$ with a strength $Q_T(\tau)$. While this is *not* a realistic representation of the spatial distribution of the heat flux induced by an individual fire to a large floor area, it does pick up two key features of such a fire. First, the overall strength of the fire (measured by its overall heat release rate) will change with time. Second, the fire will migrate from place to place as its fuel is consumed and the availability of oxygen changes with time. Under these circumstances the surface temperature distribution simplifies to:

$$\Theta(\vec{r}, \tau, 0) = \int_0^{\tau} d\tau_o \frac{Q_T(\tau_o)}{4(\pi(\tau - \tau_o))^{3/2}}\exp\left(\frac{-\eta_T^2}{4}\right) \tag{A.37}$$

$$\eta_T = \frac{\left|\vec{r} - \vec{R}(\tau_o)\right|}{\sqrt{(\tau - \tau_o)}} \tag{A.38}$$

The most relevant parts of this result in the present context are the dependence of the solution on the previous history of the surface heat flux distribution, and the fact that the Greens function G has a structure determined primarily by the similarity variable η_T which itself is inherently time dependent. Note that the singularity in the integrand at $\vec{r} = \vec{R}(\tau_o)$, $\tau = \tau_o$ is an artifact of injecting a finite heat flux into a point. The results make perfectly good sense for points away from the current location of the heat flux source.

The solution for the displacement normal to the surface can be found in an analogous manner. However, since the inversion process is somewhat more complex here a few details are provided. The Fourier–Laplace transform of the surface displacement takes the form:

$$\bar{w}(\vec{k}, p, 0) = \left(\frac{2\mu+\lambda}{\mu+\lambda}\right)\frac{\bar{Q}}{p}\left(\frac{k}{\sqrt{p+k^2}} - 1\right) \tag{A.39}$$

The solution for $w\left(\vec{r}, \tau, 0\right)$ takes the same form as Eq. (A.35) except that the Greens function $G\left(\vec{r}, \tau\right)$ is replaced by a new kernel function $K(\vec{r}, \tau)$ defined as:

$$K = \left(\frac{2\mu+\lambda}{\mu+\lambda}\right)\int_{-\infty}^{\infty}\frac{d^2\vec{k}}{(2\pi)^2}\exp\left(i\vec{k}\cdot\vec{r}\right)\oint\frac{dp}{2\pi i}\frac{\exp(p\tau)}{p} \times\left(\frac{k}{\sqrt{p+k^2}} - 1\right) \tag{A.40}$$

Carrying out the inversion of the Laplace transform first, and noting that the resulting expression depends only on $k \equiv |\vec{k}|$, the Fourier inversion integral can be reduced to:

$$K = -\left(\frac{2\mu+\lambda}{\mu+\lambda}\right)\frac{1}{2\pi\tau}\int_0^{\infty} d\xi\,\xi \;\; \mathrm{erfc}\left(\xi\right)J_0\left(\xi\eta\right), \quad \eta = \frac{r}{\sqrt{\tau}} \tag{A.41}$$

Here, J_0 denotes the Bessel function of the first kind of order zero. The final integral can be evaluated with the aid of *Mathematica* to yield:

$$K = -\left(\frac{2\mu+\lambda}{\mu+\lambda}\right)\frac{1}{8\pi\tau}\exp\left(\frac{-\eta^2}{8}\right)\left(I_o\left(\frac{\eta^2}{8}\right) - I_1\left(\frac{\eta^2}{8}\right)\right) \tag{A.42}$$

The quantities I_0 and I_1 are the modified Bessel functions of the first kind of order zero and one respectively. The minus sign in front of the (positive) expression for K arises from the definition of positive w pointing *into* the material. Thus, the thermal expansion induces a bulge out of the plane of the surface, so that w must be negative. Finally, if the heat flux to the surface is concentrated at a point as described above, the solution for the normal surface displacement becomes:

$$w = \int_0^{\tau} d\tau_o Q_T(\tau_o) K(\tau - \tau_o, \eta_T), \quad \eta_T = \frac{\left|\vec{r} - \vec{R}(\tau_o)\right|}{\sqrt{(\tau - \tau_o)}} \tag{A.43}$$

Clearly, the only significant differences between the solutions for Θ and w at the surface are in the mathematical structure of the kernel functions G and K. They are plotted in Fig. 8 in normalized form, so that the value at $\eta = 0$ for each function is one. The thermal function G has an exponential decay, consistent with the inherently transient diffusion of heat from the point source at the surface. The normal displacement kernel K however, decays algebraically with large η with $K \sim \eta^{-3}$. This is a consequence of the fact that the displacements have both equilibrium and transient components. On the other hand, the spatial dependence of both functions appears in the inherently transient independent variable $\eta = r/\sqrt{\tau}$, which describes a diffusion controlled process. Moreover, the full solutions for both the temperature and the displacement are dependent on the previous history of each quantity.

References

Abboud, N., Levy, M., Tennant, D., Mould, J., Levine, H., King, S., Ekwueme, C., Jain, A., Hart, G., 2003. Anatomy of the World Trade Center collapses: a structural engineering investigation. In: SEI/SFPE Conference on Designing Structures for Fire , Baltimore, MD, September 2003.

ANSYS Release 8.0 Documentation, ANSYS Corp., 2003.

Baum, H.R., 2005. Simulating fire effects on complex building structures. In: Gottuk, D.T., Lattimer, B.Y. (Eds.), Fire Safety Science—Proceedings of the Eighth International Symposium. International Association for Fire Safety Science, pp. 3–18.

Baum, H.R., Rehm, R.G., 2005. A simple model of the World Trade Center fireball dynamics. Proceedings of the Combustion Institute 30, 2247–2254.

Beyler, C., White, D., Peatross, M., Trellis, J., Li, S., Luers, A., Hopkins, D., 2003. Analysis of fire development in the WTC attacks. In: SEI/SFPE Conference on Designing Structures for Fire , Baltimore, MD, September 2003.

Hallquist, J.O., 1998. LS-DYNA Theoretical Manual. Livermore Software Technology Corporation, Livermore, CA, May 1998.

Hamins, A., McGrattan, K., Prasad, K., Maranghides, A., McAllister, T., 2005. Experiments and modeling of unprotected structural steel elements exposed to fire. In: Gottuk, D.T., Lattimer, B.Y. (Eds.), Fire Safety Science—Proceedings of the Eighth International Symposium. International Association for Fire Safety Science, pp. 189–200.

Hasemi, Y., 2000. Diffusion flame modeling as a basis for the rational fire safety design of built environments. In: Curtat, M. (Ed.), Fire Safety Science—Proceedings of the Sixth International Symposium. International Association for Fire Safety Science, pp. 3–21.

Hori, A., 2004. Analytical method for high temperature collapse of a 3D steel frame. Fire Science and Technology 23, 208–221.

Lane, B., 2003. A suggested cause of the fire-induced collapse of the World Trade Towers. Fire Safety Journal 38, 589–591.

McGrattan, K.B.,., 2004. Fire Dynamics Simulator (Version 4), Technical Reference Guide. NIST Special Publication 1018. National Institute of Standards and Technology, Gaithersburg, MD.

McGrattan, K.B., Bouldin, C., 2004. Simulating the fires in the World Trade Center. In: Interflam 2004. Proceedings of the Tenth International Conference , Interscience, London, 2004.

Pagni, P., 2003. Thermal glass breakage. In: Evans, D.D. (Ed.), Fire Safety Science—Proceedings of the Seventh International Symposium. International Association for Fire Safety Science, pp. 3–22.

Prasad, K., Baum, H.R., 2005. Coupled fire dynamics and thermal response of complex building structures. Proceedings of the Combustion Institute 30, 2255–2262.

Quintiere, J.G., di Marzo, M., Becker, R., 2002. A Suggested Cause of the fire-induced collapse of the World Trade Towers. Fire Safety Journal 37, 707–717.

Rehm, R.G., Pitts, W.M., Baum, H.R., Evans, D.D., Prasad, K., McGrattan, K.B., Forney, G.P., 2002. Initial Model for Fires in the World Trade Center. NISTIR 6879, third ed. National Institute of Standards and Technology, Gaithersburg, MD, pp. 699–722.

Siegel, R., Howell, J.R., 1992. Thermal Radiation Heat Transfer, third ed. Hemisphere, Washington, DC, pp. 699–722.

Sokolnikoff, I.A., 1956. Mathematical Theory of Elasticity, second ed. McGraw Hill, New York, pp. 358–367.

Thater, G., Panariello, G., Cuoco, D., 2003. World Trade Center Disaster: Damage/Debris Assessment. In: ASCE 3rd Forensics Congress , San Diego, CA, October 2003.

Usmani, A.S., Chung, Y.C., Torero, J.L., 2003. How did the WTC towers collapse: a new theory. Fire Safety Journal 38, 501–534.

Vaughan, D.K., 2002. FLEX Users Guide, Report UG8298. Weidlinger Associates Inc., Los Altos, CA, 1983 with updates through 2002.